JOURNAL OF CHEMICAL PHYSICS VOLUME 116, NUMBER 6 8 FEBRUARY 2002

ARTICLES

Surface-hopping dynamics of a spin-boson system

Donal Mac Kernan
CECAM, Ecole Normale Superieure de Lyon, 46 Allee d'Italie, 69364 Lyon Cedex 07, France

Giovanni Ciccotti
CECAM, Ecole Normale Superieure de Lyon, 46 Allee d'Italie, 69364 Lyon Cedex 07, France and INFM and Dipartimento di Fisica, Università "La Sapienza," Piazzale Aldo Moro, 2, 00185 Roma, Italy

Raymond Kapral
CECAM, Ecole Normale Superieure de Lyon, 46 Allee d'Italie, 69364 Lyon Cedex 07, France and Chemical Physics Theory Group, Department of Chemistry, University of Toronto, Toronto, ON M5S 3H6, Canada

(Received 27 August 2001; accepted 14 November 2001)

The spin-boson model is solved within the framework of quantum-classical dynamics using our recently-developed surface-hopping scheme. The quantum-classical equation of motion is expressed in an adiabatic basis and its solution is constructed from an ensemble of trajectories which undergo nonadiabatic transitions and evolve coherently on the adiabatic surfaces. Details of the algorithm for the simulation of the dynamics are presented and the method of simple Monte Carlo sampling used to evaluate the expectation values of observables is discussed. The simulation method is applied to a spin-boson system with a harmonic bath composed of ten oscillators with an Ohmic spectral density. For the spin-boson model the present implementation of quantum-classical dynamics is exact and the results of our surface-hopping simulations are in accord with previous numerically exact results for this model. © *2002 American Institute of Physics.* [DOI: 10.1063/1.1433502]

I. INTRODUCTION

Quantum-classical dynamics describes systems composed of a quantum subsystem coupled to a classical environment and provides a means to study the dynamics of many-body systems that are not amenable to investigation using full quantum dynamics.[1,2] In the quantum-classical approach we use, the isolated quantum subsystem and bath obey quantum mechanics and classical mechanics, respectively, but their coupled evolution is given by quantum-classical equations of motion where a simple Newtonian description of the environmental degrees of freedom no longer exists.[3–9] The solution of the evolution equation may be written in terms of an ensemble of surface-hopping trajectories in place of the single Newtonian trajectory of a classical system.[9,10] Other exploratory work along similar lines on a number of simple models has also appeared in the literature.[11,12] In this article we consider the application of quantum-classical dynamics to the spin-boson model.

The spin-boson system, which consists of a two-level system bilinearly coupled to a bath of harmonic oscillators, has been widely used as a simple model of an open quantum system in order to study the effects of an environment on a quantum subsystem.[13–16] This model has provided a great deal of insight into how decoherence and dissipation occur in the quantum subsystem as a result of coupling to the harmonic bath. It has also served as a testing ground for computational descriptions of many-body quantum dynamics. It is in this connection that we explore the dynamics of this system.

In an earlier paper[9] we wrote the solution of the quantum-classical evolution equation, expressed in an adiabatic basis, as an integral equation. This integral equation was solved by iteration to yield a series whose terms were ordered by the number of nonadiabatic transitions. A hybrid Molecular Dynamics (MD)-Monte Carlo (MC) scheme was constructed to solve the integral equation. In this scheme, quantum transitions and the times at which they occur are sampled using Monte Carlo methods. The evolution between such quantum transition events is carried out using classical molecular dynamics, either on a single adiabatic surface, if the evolution for that time segment involves a diagonal element of the density matrix, or on the mean of two coherently coupled adiabatic surfaces, if evolution involves an off-diagonal element of the density matrix. This surface-hopping method is a formally exact solution of the quantum-classical equations of motion and differs from other surface-hopping methods that have been developed recently.[17–19] Implementation of our formally exact surface-hopping scheme entails a finite-difference approximation to a momentum derivative operator that is responsible for momentum changes in the bath induced by quantum transitions. A "momentum-jump" approximation may be made which reduces the action of this term to bath momentum translations. Thus far, this method of solution, in its exact and approximate momentum-jump forms, has been applied to model systems where the "bath" consists of a single classical harmonic or anharmonic oscillator.[10]

The goals and main results of this study are as follows:

First we apply the hybrid MD-MC scheme to the spin-boson system and demonstrate the utility of the method for the study of systems with many-body baths. Since the present quantum-classical and full quantum dynamics are equivalent for the spin-boson model, we may compare the results of our quantum-classical simulation method with known results for this system obtained using other quantum mechanical simulation techniques. Second, our calculations on the spin-boson model are used to demonstrate the feasibility of the hybrid MD-MC scheme and assess its convergence properties. Finally, we investigate the validity of the momentum-jump approximation for nonadiabatic transitions and momentum exchanges with the bath. We show that for the spin-boson system this approximation is very accurate. We also show that the momentum-jump approximation can be generalized so that the exact operator responsible for nonadiabatic transitions can be written as a sum of momentum-jump operators. Since this approximation considerably simplifies the dynamics such tests are important for future applications.

The outline of the paper is as follows: In Sec. II we present the quantum-classical evolution equations and the algorithm for their solution. In particular, we describe how the operator that is responsible for nonadiabatic transitions can be implemented and how simple Monte Carlo sampling can be carried out to evaluate the time and phase space integrals that enter the solution. Section III defines the spin-boson model and gives the simulation details needed for its solution by the surface-hopping algorithm. In this section we also show that the present quantum-classical equations of motion are exact for the spin-boson model. The numerical results of the study are presented in Sec. IV. We solve the quantum-classical evolution equation for the spin-boson model with an Ohmic spectral density using a surface-hopping scheme and compare our results with existing numerically exact solutions of this model.[20,21] The conclusions are given in Sec. V.

II. QUANTUM-CLASSICAL DYNAMICS

The starting point for the calculations presented in this paper is the quantum-classical Liouville equation,[3–9]

$$\begin{aligned}\frac{\partial\rho_W(R,P,t)}{\partial t}&=-\frac{i}{\hbar}[\hat{H}_W,\hat{\rho}_W(t)]\\&\quad+\frac{1}{2}(\{\hat{H}_W,\hat{\rho}_W(t)\}-\{\hat{\rho}_W(t),\hat{H}_W\})\\&=-i\hat{\mathcal{L}}\hat{\rho}_W(R,P,t),\end{aligned} \tag{1}$$

which describes the evolution of the density matrix $\hat{\rho}_W(R,P,t)$ for a quantum subsystem composed of particles with mass m coupled to a classical bath of particles with mass M. The subscript W derives from the fact that this equation was obtained by taking the partial Wigner transform[22] over the bath degrees of freedom and expanding the evolution operator in powers of $(m/M)^{1/2}$. Reference 9 should be consulted for a derivation of Eq. (1) and a discussion of its solution by surface-hopping methods. Quantities such as the density matrix or Hamiltonian $\hat{H}_W=\hat{H}_W(R,P)$ depend on the classical phase space coordinates of the N-particle bath $(R,P)=(R_1,R_2,\ldots,R_N,P_1,P_2,\ldots,P_N)$, while a hat is used to denote the fact that they are abstract operators in the Hilbert space of the quantum subsystem. More explicitly, the Hamiltonian is defined by

$$\hat{H}_W=\frac{P^2}{2M}+\frac{\hat{p}^2}{2m}+\hat{V}_W(\hat{r},R), \tag{2}$$

with $\hat{p}$ and $\hat{r}$ the momentum and position operators for the quantum subsystem, while the potential energy operator $\hat{V}_W(\hat{r},R)$ may be decomposed into quantum subsystem, classical bath and coupling contributions,

$$\hat{V}_W(\hat{r},R)=\hat{V}_s(\hat{r})+V_b(R)+\hat{V}_c(\hat{r},R). \tag{3}$$

The last line of Eq. (1) defines the quantum-classical Liouville operator.

While Eq. (1) may be studied in any basis, it is especially convenient to represent this equation in an adiabatic basis if its solution is constructed by a surface-hopping algorithm. The adiabatic eigenstates $|\alpha;R\rangle$ are parametrized by the classical coordinates and are the solutions of the eigenvalue problem, $\hat{h}_W|\alpha;R\rangle=E_\alpha(R)|\alpha;R\rangle$, where $\hat{h}_W(R)=(\hat{p}^2/2m)+\hat{V}_W(\hat{r},R)$. In this basis any operator $\hat{O}_W$ has matrix elements $O_W^{\alpha\alpha'}=\langle\alpha;R|\hat{O}_W|\alpha';R\rangle$. The $\mathbf{O}_W$ matrix may be written as a vector with components O_W^s by associating an index $s=\alpha\mathcal{N}+\alpha'$ with the pair $(\alpha\alpha')$, where $0\leqslant\alpha,\alpha'<\mathcal{N}$ for an $\mathcal{N}$-state quantum subsystem.

Using this notation and introducing a subscript to label different values of s, e.g., $s_k=\alpha_k\mathcal{N}+\alpha_k'$, the quantum-classical Liouville equation has the form[9,10]

$$\frac{\partial\rho_W^{s_j}(R,P,t)}{\partial t}=\sum_{s_k}-i\mathcal{L}_{s_js_k}\rho_W^{s_k}(R,P,t). \tag{4}$$

The matrix elements of the quantum-classical Liouville operator can be found in Refs. 9 and 10 and are given by

$$-i\mathcal{L}_{s_js_k}=-(i\omega_{s_j}+iL_{s_j})\delta_{s_js_k}+J_{s_js_k}. \tag{5}$$

The diagonal term $-(i\omega_{s_j}+iL_{s_j})\delta_{s_js_k}$ contains the frequency $\omega_{s_j}(R)=(E_{\alpha_j}(R)-E_{\alpha_j'}(R))/\hbar$ and the classical Liouville operator L_{s_j},

$$iL_{s_j}=\frac{P}{M}\cdot\frac{\partial}{\partial R}+\frac{1}{2}(F_W^{\alpha_j}+F_W^{\alpha_j'})\cdot\frac{\partial}{\partial P}, \tag{6}$$

where the Hellmann–Feynman force $F_W^{\alpha_j}=-\langle\alpha_j;R|\,\partial\hat{V}_W(\hat{r},R)/\partial R\,|\alpha_j;R\rangle$. The term $J_{s_js_k}$ is responsible for nonadiabatic transitions and has the form

$$\begin{aligned}J_{s_js_k}=&-\frac{P}{M}\cdot d_{\alpha_j\alpha_k}\left(1+\frac{1}{2}S_{\alpha_j\alpha_k}\cdot\frac{\partial}{\partial P}\right)\delta_{\alpha_j'\alpha_k'}\\&-\frac{P}{M}\cdot d^*_{\alpha_j'\alpha_k'}\left(1+\frac{1}{2}S^*_{\alpha_j'\alpha_k'}\cdot\frac{\partial}{\partial P}\right)\delta_{\alpha_j\alpha_k},\end{aligned} \tag{7}$$

where $S_{\alpha_j\alpha_k}=(E_{\alpha_j}-E_{\alpha_k})d''_{\alpha_j\alpha_k}(P/M)\cdot d_{\alpha_j\alpha_k})^{-1}$ and $d_{\alpha_j\alpha_k}=\langle\alpha_j;R|\partial/\partial R\,|\alpha_k;R\rangle$ is the nonadiabatic coupling matrix element which determines the nonadiabaticity of the system and can be considered to be a small expansion parameter.

Henceforth, we choose a real adiabatic basis so that $d_{\alpha\alpha}=0$ and $J_{s_js_k}$ is off-diagonal. Moreover, when the first term on the right hand side of Eq. (7) is nonzero, the second term is zero, and vice versa. Specifically, the first term is nonzero for values of s_j and s_k such that $s_j-s_k=\pm l\mathcal{N}$, while the second term is nonzero only if $s_j-s_k=\pm l$, where $1\leq l<\mathcal{N}$. These two conditions restrict the sequences of transitions that can occur and so determine the structure of the nonadiabatic transition matrix **J**, which we may now write as

$$J_{s_js_k}=\mathcal{J}^0_{s_js_k}\delta_{s_j,s_k\pm l\mathcal{N}}+\mathcal{J}^1_{s_js_k}\delta_{s_j,s_k\pm l}, \tag{8}$$

where $\mathcal{J}^{\kappa}_{s_js_k}$ (κ=0,1), correspond, respectively, to the first and second terms in Eq. (7) multiplying the delta functions. For instance, for a two-state quantum subsystem, **J** takes the form

$$\mathbf{J}=\begin{pmatrix} 0 & \mathcal{J}^1_{01} & \mathcal{J}^0_{02} & 0 \\ \mathcal{J}^1_{10} & 0 & 0 & \mathcal{J}^0_{13} \\ \mathcal{J}^0_{20} & 0 & 0 & \mathcal{J}^1_{23} \\ 0 & \mathcal{J}^0_{31} & \mathcal{J}^1_{32} & 0 \end{pmatrix}. \tag{9}$$

To compute the action of the elements of **J**, we must consider how to evaluate the effect of differential operators like $(1+\frac{1}{2}S_{\alpha_j\alpha_k}\cdot(\partial/\partial P))$ on functions of the classical phase space coordinates. The most straightforward way to compute the momentum derivative is by finite differences but this may be subject to numerical instabilities. Alternatively, one may make the momentum-jump approximation[9] and write this operator as

$$1+\frac{1}{2}S_{\alpha_j\alpha_k}\cdot\frac{\partial}{\partial P}\approx e^{(1/2)S_{\alpha_j\alpha_k}\cdot(\partial/\partial P)}, \tag{10}$$

which simply induces a shift in the bath momentum. Both of these schemes were used in our earlier studies of a two-level system coupled to a single classical oscillator.[10]

It is possible to generalize the momentum-jump approximation to the operator **J**. In particular, $1+z$ may be written as

$$1+z=e^z+\mathcal{O}(z^2) \tag{11}$$

$$=1+\tfrac{1}{2}(e^z-e^{-z})+\mathcal{O}(z^3). \tag{12}$$

These formulas can be extended to higher order at the price of introducing complex arguments. The general formula is

$$1+z=e^z-\sum_{k=2}^{\infty}\chi_k(z), \tag{13}$$

where

$$\chi_k(z)=\frac{1}{k}\sum_{l=1}^{k}e^{r(l,k)z}-1, \tag{14}$$

and $r(l,k)=e^{2\pi il/k}$ are the kth roots of unity. This result can be established by Taylor expanding the right-hand side of Eq. (13), identifying the coefficients of powers of z and using known algebraic properties of the roots of unity. Although difficult to apply beyond second order, this formula provides a systematic way to apply the momentum jump approximation to any order and determine the accuracy of low-order approximations.

We may now construct a sequence of approximations to $(1+\frac{1}{2}S_{\alpha_j\alpha_k}\cdot(\partial/\partial P))$. The action of this operator on any phase space function $f(R,P)$ using the first approximation in Eq. (11) is given by

$$\begin{aligned}\left(1+\frac{1}{2}S_{\alpha_j\alpha_k}\cdot\frac{\partial}{\partial P}\right)f(R,P)&=e^{(1/2)S_{\alpha_j\alpha_k}\cdot(\partial/\partial P)}f(R,P)+\mathcal{O}(S^2_{\alpha_j\alpha_k})\\&=f(R,P+\tfrac{1}{2}S_{\alpha_j\alpha_k})+\mathcal{O}(S^2_{\alpha_j\alpha_k}).\end{aligned} \tag{15}$$

This is just the momentum jump approximation introduced earlier.[9] The second approximation obtained using Eq. (12) is

$$\begin{aligned}\left(1+\frac{1}{2}S_{\alpha_j\alpha_k}\cdot\frac{\partial}{\partial P}\right)f(R,P)&=(1+\tfrac{1}{2}(e^{(1/2)S_{\alpha_j\alpha_k}\cdot(\partial/\partial P)}-e^{-(1/2)S_{\alpha_j\alpha_k}\cdot(\partial/\partial P)}))\\&\quad\times f(R,P)+\mathcal{O}(S^3_{\alpha_j\alpha_k})\\&=f(R,P)+\tfrac{1}{2}(f(R,P+\tfrac{1}{2}S_{\alpha_j\alpha_k})\\&\quad-f(R,P-\tfrac{1}{2}S_{\alpha_j\alpha_k}))+\mathcal{O}(S^3_{\alpha_j\alpha_k}),\end{aligned} \tag{16}$$

and will be termed the second order jump approximation. In realizations of quantum-classical dynamics involving n nonadiabatic transitions, the first order jump approximation yields a single trajectory with momentum jumps. In second (and higher) order a branching tree of trajectories is spawned. For instance, using the second order approximation 3^n trajectories will be produced in each realization of the evolution.

Making use of the Dyson equation and the fact that the first term in the quantum-classical Liouville operator is diagonal, the evolution Eq. (4) may be written in integral form as[9,10]

$$\begin{aligned}\rho^{s_0}_W(R,P,t)&=e^{-(i\omega_{s_0}+iL_{s_0})t}\rho^{s_0}(R,P,0)\\&\quad+\sum_{s_1}\int_0^t dt'\,e^{-(i\omega_{s_0}+iL_{s_0})(t-t')}\\&\quad\times J_{s_0s_1}\rho^{s_1}_W(R,P,t').\end{aligned} \tag{17}$$

We may simplify this equation by defining

$$\begin{aligned}U^{\dagger}_{s_k}(t_k-t_{k+1})&=e^{-(i\omega_{s_k}+iL_{s_k})(t_k-t_{k+1})}\\&=e^{-i\int_{t_k}^{t_{k+1}}d\tau\,\omega_{s_k}(R^{t_k}_{s_k,\tau})}e^{-iL_{s_k}(t_k-t_{k+1})}\\&\equiv\mathcal{W}_{s_k}(t_k,t_{k+1})e^{-iL_{s_k}(t_k-t_{k+1})},\end{aligned} \tag{18}$$

where the time-reversed phase point under the classical evolution operator L_{s_k} is denoted by

$$(R^{t_k}_{s_k,t_{k+1}},P^{t_k}_{s_k,t_{k+1}})=e^{-iL_{s_k}(t_k-t_{k+1})}(R,P)\,. \tag{19}$$

Using this notation and iterating the integral equation to obtain its solution we find

$$\rho_W^{s_0}(R,P,t)=U_{s_0}^{\dagger}(t)\rho^{s_0}(R,P,0)+\sum_{n=1}^{\infty}\sum_{s_1\cdots s_n}\int_0^{t_0}dt_1\int_0^{t_1}dt_2 \cdots\int_0^{t_{n-1}}dt_n\prod_{k=1}^{n}[U_{s_{k-1}}^{\dagger}(t_{k-1}-t_k)J_{s_{k-1}s_k}] \times U_{s_n}^{\dagger}(t_n)\rho^{s_n}(R,P,0), \tag{20}$$

where $t_0=t$. This recursive formula allows one to compute the terms in the integral equation solution in a systematic fashion.

In order to complete the calculation of the nth order term in Eq. (20) we must decide how to carry out the sums over the discrete s_k indices and how to perform the multiple time integrals. For the first problem, not all the sequences $\{s_0,\ldots,s_n\}$ contribute since only a subset $\mathcal{S}$ of the sequences is physically permissible. From the discussion of **J** above the allowed sequences have $s_k-s_{k+1}=\pm l\mathcal{N}$ or $s_k-s_{k+1}=\pm l$ for $1\leqslant l<\mathcal{N}$. One can either count all the elements of $\mathcal{S}$ contributing to Eq. (20), or if there are too many elements, one may approximate the sum through a Monte Carlo sampling of the summand over $\mathcal{S}$.

For the second problem, Monte Carlo techniques must be used, the simplest involving uniform sampling to evaluate the time integrals. The time integrals that must be computed are of the type,

$$\mathcal{I}=\int_0^{t_0}dt_1\int_0^{t_1}dt_2\cdots\int_0^{t_{n-1}}dt_n f(t_1,t_2,\ldots,t_n). \tag{21}$$

When the integrand is invariant under permutations of its arguments, it is a simple matter to reduce such an integral to an integral over a hypercube; however, the reduction is more generally valid since the change of variables $u_l=(t_l/t_{l-1})^{n-l+1}$, where $u_l\in[0,1]$ for $1\leqslant l\leqslant n$, with the jacobian $J(u_1,\ldots,u_n;t_0)=t_0^n/n!$, independent of the integration variables, reduces this integral to

$$\mathcal{I}=\frac{t_0^n}{n!}\int_0^1du_1\int_0^1du_2\cdots\int_0^1du_n f(t_1(u),t_2(u),\ldots,t_n(u)). \tag{22}$$

The integral (22) can be estimated by a simple uniform Monte Carlo sampling. One way to generate uniformly distributed random numbers is through a standard pseudorandom number generator. However, for finite sequences, clustering of numbers is known to occur. Another way to produce the desired time sequences is through quasirandom numbers, also called least discrepancy sequences.[23] Such sequences do not exhibit the clustering of random numbers and when used to evaluate multi-dimensional integrals typically converge far more quickly. We have used this method to obtain the results in this paper.

There is one final issue to consider. Most often one is not interested in the computation of the density matrix itself but in expectation values of observables. In this case we must compute

$$\begin{aligned}\overline{O}(t)&=\mathrm{Tr}'\int dRdP\hat{O}_W(R,P)\hat{\rho}_W(R,P,t)\\&=\mathrm{Tr}'\int dRdP(e^{i\hat{\mathcal{L}}t}\hat{O}_W(R,P))\hat{\rho}_W(R,P,0)\\&=\mathrm{Tr}'\int dRdP\hat{O}_W(R,P,t)\hat{\rho}_W(R,P,0),\end{aligned} \tag{23}$$

where Tr′ denotes a trace over the quantum subsystem. In the second line of Eq. (23) we moved the time evolution operator from the density matrix to the observable. Given that the formal solution for the time evolution of an observable is

$$\hat{O}_W(R,P,t)=e^{i\hat{\mathcal{L}}t}\hat{O}_W(R,P), \tag{24}$$

its solution as series may be found by carrying out an analysis like that leading to Eq. (20). The result is

$$O_W^{s_0}(R,P,t)=U_{s_0}(t)O^{s_0}(R,P,0) +\sum_{n=1}^{\infty}(-1)^n\sum_{s_1\cdots s_n}\int_0^{t_0}dt_1\int_0^{t_1}dt_2 \cdots\int_0^{t_{n-1}}dt_n\prod_{k=1}^{n}[U_{s_{k-1}}(t_{k-1}-t_k)J_{s_{k-1}s_k}] \times U_{s_n}(t_n)O^{s_n}(R,P,0), \tag{25}$$

with $t_0=t$ and where

$$\begin{aligned}U_{s_k}(t_k-t_{k+1})&=e^{(i\omega_{s_k}+iL_{s_k})(t_k-t_{k+1})}\\&=e^{i\int_{t_k}^{t_{k+1}}dt'\,\omega_{s_k}(\overline{R}^{t_k}_{s_k,t'})}e^{iL_{s_k}(t_k-t_{k+1})}\\&\equiv\overline{\mathcal{W}}_{s_k}(t_k-t_{k+1})e^{iL_{s_k}(t_k-t_{k+1})},\end{aligned} \tag{26}$$

and the classical evolution operator $\exp(iL_{s_k}(t_k-t_{k+1}))$ now evolves phase points forward in time,

$$(\overline{R}^{t_k}_{s_k,t_{k+1}},\overline{P}^{t_k}_{s_k,t_{k+1}})=e^{iL_{s_k}(t_k-t_{k+1})}(R,P)\,. \tag{27}$$

The phase space integrals in Eq. (23) were computed using importance sampling based on $\hat{\rho}_W(R,P,0)$. We have made use of this formulation to obtain the results given below.

III. SPIN-BOSON MODEL AND SIMULATION DETAILS

The spin-boson Hamiltonian, which describes a two-level system, with states $\{|\uparrow>,|\downarrow>\}$, bilinearly coupled to a harmonic bath of N oscillators with masses M_j and frequencies ω_j, may be written as

$$\hat{H}=-\hbar\Omega\hat{\sigma}_x+\sum_{j=1}^{N}\left(\frac{\hat{P}_j^2}{2M_j}+\frac{1}{2}M_j\omega_j^2\hat{R}_j^2-c_j\hat{R}_j\hat{\sigma}_z\right). \tag{28}$$

Here $2\hbar\Omega$ is the energy gap of the isolated two-state system and

$$\hat{\sigma}_x=\begin{pmatrix}0&1\\1&0\end{pmatrix},\quad \hat{\sigma}_z=\begin{pmatrix}1&0\\0&-1\end{pmatrix}, \tag{29}$$

are the Pauli spin matrices. To fix the values of the parameters in this N-oscillator spin-boson model, we have chosen to employ the forms of the coupling constants c_j and frequencies ω_j introduced by Makri and Thompson,[21]

$$c_j=\sqrt{\xi\hbar\omega_0 M_j}\,\omega_j\,,\qquad \omega_j=-\omega_c\ln\left(1-j\frac{\omega_0}{\omega_c}\right),\tag{30}$$

where

$$\omega_0=\frac{\omega_c}{N}\left(1-e^{-\omega_{\max}/\omega_c}\right).\tag{31}$$

This choice corresponds to the most efficient way to represent an infinite bath with Ohmic spectral density by a finite number of oscillators. The spectral density is characterized by the Kondo parameter ξ and frequency ω_c. The parameter $\omega_{\max}$ is a cutoff frequency.

Although we are not specifically concerned here with the physics of the dynamics of a quantum subsystem coupled to a thermal bath, we use this set of parameters since it provides us with a convenient means to compare our surface-hopping results with the exact numerical results of Makri and Thompson on the N-oscillator spin-boson model.

Taking the partial Wigner transform[22] over the bath degrees of freedom, the Hamiltonian becomes

$$\begin{aligned}\hat H_W&=-\hbar\Omega\hat\sigma_x+\sum_{j=1}^{N}\left(\frac{P_j^2}{2M_j}+\frac12 M_j\omega_j^2R_j^2-c_jR_j\hat\sigma_z\right)\\&=\hat h_s+H_b+\hat V_c(R),\end{aligned}\tag{32}$$

which depends on the classical phase space coordinates (R,P) and the spin degrees of freedom. The second line of Eq. (32) defines the subsystem Hamiltonian $\hat h_s=-\hbar\Omega\hat\sigma_x$, the bath Hamiltonian $H_b(R,P)=\Sigma_{j=1}^{N}(P_j^2/2M_j+\frac12 M_j\omega_j^2R_j^2)=\Sigma_{j=1}^{N}(P_j^2/2M_j)+V_b(R)$ and the coupling potential energy $\hat V_c(R)=-\Sigma_{j=1}^{N}c_jR_j\hat\sigma_z\equiv\gamma(R)\hat\sigma_z$.

We now establish that the approximate quantum-classical evolution is exact for this Hamiltonian, i.e., it is identical with the full quantum evolution. The quantum mechanical density matrix satisfies the von Neumann equation,

$$\frac{\partial\hat\rho(t)}{\partial t}=-\frac{i}{\hbar}[\hat H,\hat\rho(t)],\tag{33}$$

and its partial Wigner transform is[25]

$$\frac{\partial\hat\rho_W(R,P,t)}{\partial t}=-\frac{i}{\hbar}\left(\hat H_We^{\hbar\Lambda/2i}\hat\rho_W(t)-\hat\rho_W(t)e^{\hbar\Lambda/2i}\hat H_W\right),\tag{34}$$

where $\Lambda=\overleftarrow{\nabla}_P\cdot\overrightarrow{\nabla}_R-\overleftarrow{\nabla}_R\cdot\overrightarrow{\nabla}_P$. One may easily verify that only the first order terms in the expansion of the exponential operator, $e^{\hbar\Lambda/2i}=1+\hbar\Lambda/2i$, contribute to the right-hand side of Eq. (34) in view of the fact that $H_b(R,P)$ is a simple phase space function of its arguments depending quadratically on R and P and the coupling term is linear in R. In this case Eq. (34) reduces to the quantum-classical Liouville equation and thus, as stated, for the spin-boson model the evolution is given exactly by Eq. (1).

In the calculations presented below we shall use dimensionless variables defined by

$$R_j'=\left(\frac{M_j\omega_c}{\hbar}\right)^{1/2}R_j\,,\qquad P_j'=(\hbar M_j\omega_c)^{-1/2}P_j\,.\tag{35}$$

The Hamiltonian then takes the form,

$$\hat H_W'=\frac{\hat H_W}{\hbar\omega_c}=-\Omega'\hat\sigma_x+\sum_j\left(\frac{P_j'^2}{2}+\frac12\omega_j'^2R_j'^2-c_j'\hat\sigma_zR_j'\right),\tag{36}$$

where

$$\Omega'=\frac{\Omega}{\omega_c},\qquad \omega_j'=\frac{\omega_j}{\omega_c},\qquad c_j'=\sqrt{\xi\frac{\omega_0}{\omega_c}}\,\omega_j'\,.\tag{37}$$

Below we shall also require the dimensionless temperature parameter $\beta'=\hbar\omega_c\beta=\hbar\omega_c/(k_BT)$ and the dimensionless time $t'=t\omega_c$. Henceforth, when there is no ambiguity, we shall drop the primes but dimensionless variables are to be understood.

The solution of the integral equation for the density matrix elements in the adiabatic basis in Eq. (20) involves the adiabatic energies $E_\alpha(R)$, (α=0,1), which are the eigenvalues of $\hat h_W(R)=\hat h_s+V_b(R)+\hat V_c(R)$ and are given by

$$E_{0,1}(R)=V_b(R)\mp\sqrt{\Omega^2+\gamma(R)^2}.\tag{38}$$

The corresponding eigenvectors are

$$\frac{1}{\sqrt{2(1+G^2)}}\begin{pmatrix}1+G\\1-G\end{pmatrix},\qquad\frac{1}{\sqrt{2(1+G^2)}}\begin{pmatrix}G-1\\1+G\end{pmatrix},\tag{39}$$

where

$$G(R)=\frac{1}{\gamma(R)}\left[-\Omega+\sqrt{\Omega^2+\gamma(R)^2}\right].\tag{40}$$

The classical Liouville operator iL_{s_k} and $J_{s_js_k}$ involve the diagonal and off-diagonal Hellmann–Feynman forces which, for the spin-boson model, can be computed easily from the quantities given above.

In the calculations presented below we have assumed an initially uncorrelated density matrix where the subsystem is in state $|\uparrow\rangle$ and bath is in thermal equilibrium, so that the initial density matrix has the form,

$$\hat\rho(0)=\hat\rho_s(0)Z_b^{-1}e^{-\beta\widehat{H_b}},\qquad\hat\rho_s(0)=\begin{pmatrix}1&0\\0&0\end{pmatrix},\tag{41}$$

where Z_b is the bath partition function. The partial Wigner transform of this initial density operator is[22]

$$\hat\rho_W(R,P,0)=\hat\rho_s(0)\rho_{bW}(R,P),\tag{42}$$

where, in dimensionless variables,

$$\begin{aligned}\rho_{bW}(R,P)=\prod_{i=1}^{N}&\frac{\tanh(\beta\omega_i/2)}{\pi}\\&\times\exp\left[-\frac{2\tanh(\beta\omega_i/2)}{\omega_i}\left(\frac{P_i^2}{2}+\frac{\omega_i^2R_i^2}{2}\right)\right].\end{aligned}\tag{43}$$

In order to compare our results with those in the literature we focus our attention on the computation of the expectation value of the observable

$$\hat O=\hat\sigma_z=\begin{pmatrix}1&0\\0&-1\end{pmatrix},\tag{44}$$

whose average is the population difference in the quantum subsystem.

IV. RESULTS

For the spin-boson model the Feynman–Vernon influence functional technique[24] provides an elegant starting point for investigations of the dynamics. Various treatments based on this approach have appeared in the literature.[13–16] In this study we used the exact numerical results on a spin-boson system with a finite number of oscillators[21] obtained by employing an iterative path integral methodology developed by Makri and co-workers[20] as a basis for comparison with the results of our surface-hopping scheme.

The dynamics of the spin-boson model with Ohmic spectral density is characterized by the dimensionless parameters Ω, $\omega_{\max}$ and ξ. The statistical behavior of this model stems from the form chosen for the initial-time density matrix in Eq. (42) which depends on the additional parameter β. The system parameters used in this study were $\Omega=1/3$ and $\omega_{\max}=3$, while the Kondo parameter and reduced temperature took the two sets of values ($\xi=0.007$, $\beta=0.3$) and ($\xi=0.1$, $\beta=3.0$). The harmonic bath consisted of ten oscillators. While Makri and Thompson[21] have shown that ten harmonic oscillators can mimic an infinite dimensional bath and used this discrete model to study the dynamics of the thermalization of the two-level quantum subsystem, we employed this number of oscillators and their parameterization in our calculations simply to compare with their exact results. Consequently, we have explored a range of coupling strengths for which a significant degree of nonadiabaticity is present, without studying the full range of physically relevant values of the friction.

Before presenting the comparison of the influence functional and surface-hopping results, we examine various possible choices for the numerical implementation of the nonadiabatic transition operator $J_{s_j s_k}$. As discussed in Sec. II, the action of $J_{s_j s_k}$ may be computed using either a finite-difference scheme or various orders of the jump approximation. For this purpose we have checked the precision with which we can perform the dynamical evolution by examining the phase space observable $\overline{O}(t) \equiv \mathrm{Tr}'\int dRdP\hat{O}_W(R,P,t)\hat{\rho}_s(0)\rho_{bW}(R,P)$. In Fig. 1 we plot $\overline{O}(t)$ versus time and show that the finite difference and first and second order jump approximations are in accord for the entire simulation time. This agreement is model dependent and for other models larger differences have been observed.[10]

We have also examined how well the computed evolution satisfies the conservation laws of the model. In particular, we have verified that the norm of the initial density operator and the expectation value of the Hamiltonian $\hat{H}_W$ are well conserved. As examples, in Fig. 2 we show $\overline{H_W}(R,P,t)=\mathrm{Tr}'\,\hat{H}_W(R,P,t)\hat{\rho}_s(0)$ versus time for a given phase space point (R,P) as well as its phase space average $\overline{H}(t)$. One can see that both quantities are conserved to a high degree of accuracy.

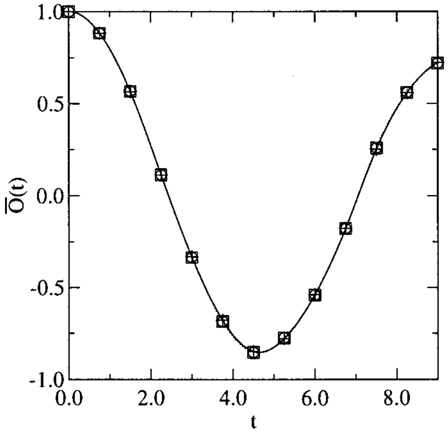

FIG. 1. Time dependence of $\overline{O}(t)$ using finite-difference (+), first order jump (□), and second order jump (○) approximations to $J_{s_j s_k}$ for $\xi=0.007$, including up to two nonadiabatic transitions. The solid lines in this and the following figures are polynomial fits to the data points as guides the eye.

We now compare our surface-hopping results with the known numerically exact results for this model. Since the first order jump approximation was shown to be accurate we have used this expression to evaluate $J_{s_j s_k}$. Figure 3 is a plot of $\overline{O}(t)$ versus time computed using the surface-hopping algorithm including up to four $(n=4)$ nonadiabatic transitions along with the influence functional results for a Kondo parameter of $\xi=0.007$. One can see that for the time interval shown our results for $n=4$ are in complete accord with those of Makri and Thompson.[21] It is instructive to examine the individual adiabatic and nonadiabatic contributions to the surface-hopping solution as a function of time. These results are shown in Fig. 4. While the coupling to the bath is quite weak and adiabatic dynamics dominates the structure for this value of the Kondo parameter, the dynamics has nonnegligible nonadiabatic components. The convergence of the surface-hopping results may also be gauged from an examination of this figure: the third and fourth order contributions are small over the entire time interval studied.

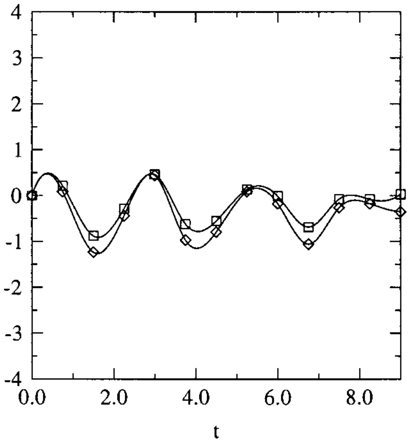

FIG. 2. Plots of $\overline{H_W}(R,P,t)$ for a given phase space point (R,P) and its phase space average $\overline{H}(t)$ vs time. (□), $(\overline{H_W}(R,P,t)-\overline{H_W}(R,P,0))\times 10^5/\overline{H_W}(R,P,0)$; (◇), $(\overline{H}(t)-\overline{H}(0))\times 10^7/\overline{H}(0)$, where $\overline{H_W}(R,P,0)=30.278\,072$ and $\overline{H}(0)=33.654\,133$.

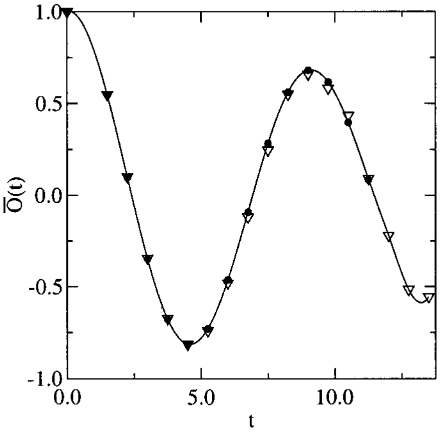

FIG. 3. $\overline{O}(t)$ vs time for ξ=0.007. Influence functional results (●) (see text), surface-hopping results for n up to 4 (▽).

Figures 5 and 6 present the results for a stronger subsystem–bath coupling strength, ξ=0.1, where the nonadiabatic contributions are even more significant. The surface-hopping results compare favorably with the influence functional results. They are almost indistinguishable from the exact Feynman–Vernon influence functional results of Makri and Thompson (Fig. 5). The decomposition into adiabatic and nonadiabatic contributions is presented in Fig. 6 and shows that substantial nonadiabatic effects exist and adiabatic dynamics is poor approximation to the true dynamics. In the figure we can also see that the $n=5$ and $n=6$ nonadiabatic contributions are small up to approximately $t=5$ and are significant for times greater than $t=7$, indicating that for longer times nonadiabatic contributions with $n>6$ must be included to achieve convergence.

The time scale for the decay of the observable $\overline{O}(t)$ depends on the magnitude of the Kondo parameter. Our calculations explored weak to moderate values of this coupling parameter and intermediate times. For fairly weak coupling (ξ=0.007) decay occurs over several oscillation periods, while for moderate coupling strengths (ξ=0.1) the decay is much faster. Our results are restricted to roughly one period, for the period of the oscillation considered in the simulation.

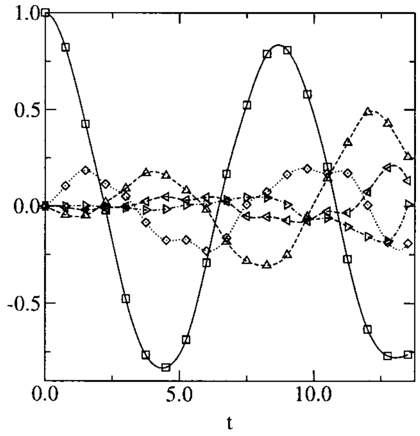

FIG. 4. Contributions to $\overline{O}(t)$ vs time for ξ=0.007. Individual contributions are: adiabatic dynamics, $n=0$, (□); nonadiabatic contributions, $n=1$, (◇); $n=2$, (△); $n=3$, (◁); $n=4$, (▷).

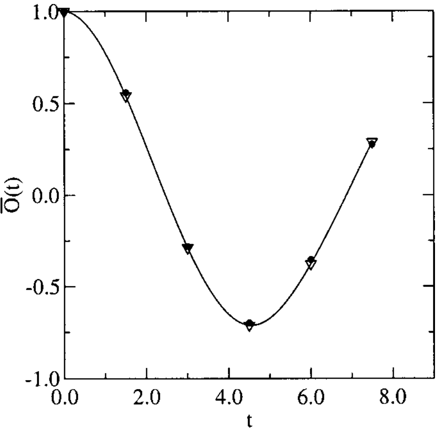

FIG. 5. $\overline{O}(t)$ vs time for ξ=0.1. Comparison of surface-hopping (n up to 6) (▽) and exact influence functional (●) (see text) results.

V. CONCLUSION

The results presented in this paper demonstrated that quantum-classical equations of motion can be solved accurately using a surface-hopping algorithm for a quantum subsystem interacting with a many-body bath. In addition to confirming the ability of the method to correctly describe the dynamics of the spin-boson model by comparison with numerically accurate results for this system, a number of additional features have been incorporated into the surface-hopping algorithm. The operator **J** plays an important role in quantum-classical dynamics since it accounts for nonadiabatic transitions and momentum transfer to and from the bath. We have presented a systematic way to evaluate this operator in a numerically stable fashion by a hierarchy of momentum-jump approximations involving only momentum translation operators, instead of a less stable finite difference approximation to the momentum derivatives appearing in this operator.

One of the principal motivations for developing a quantum-classical description is to be able to treat the dynamics of a many-body environment interacting with a quantum subsystem in a detailed fashion. Even for the extensively-studied spin-boson model, interesting informa-

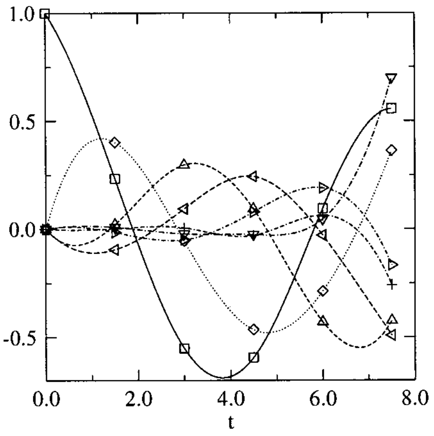

FIG. 6. Decomposition of $\overline{O}(t)$ for ξ=0.1 into adiabatic and individual nonadiabatic contributions: $n=0$, (□); nonadiabatic contributions, $n=1$, (◇); $n=2$, (△); $n=3$, (◁); $n=4$, (▷); $n=5$, (▽); $n=6$, (+).

tion on the dynamics of the bath and its equilibrium time correlation functions remains to be extracted. Since our solution method provides a dynamical description of the bath in terms of an ensemble of coherently evolving surface-hopping trajectories, both quantum subsystem and bath dynamical correlation functions can be computed directly using this ensemble. The transport properties of the system expressed in terms of equilibrium time correlation functions allow one to explore the validity of quantum-classical dynamics as well as the utility of the simulation algorithm for the dynamics.[25]

The present results provide the background for applications of quantum-classical methods to the calculation of statistical mechanical averages and dynamical properties of realistic systems of chemical and physical interest. Since our surface-hopping scheme uses classical bath trajectories, in principle, the extension to complex molecular condensed phase baths does not introduce difficulties. The computational penalty simply stems from the heavier CPU load needed to integrate the classical trajectory segments. The current formulation of the method is restricted to systems where relatively few nonadiabatic transitions are necessary to describe the phenomena. This limitation arises from the fact that the number of points needed to evaluate the time integrals by Monte Carlo sampling is large and the integrands tend to oscillate. This difficulty can be overcome partially by using more sophisticated Monte Carlo sampling that goes beyond the simple sampling scheme used here. Another way to extend the calculations to higher orders is to implement some form of decoherence into the scheme so that multidimensional time integrals of high order do not contribute. Both of these methods are under investigation. In its current form, our simulation method should be directly applicable to the study of rapidly decaying correlation functions in real many-body systems.

ACKNOWLEDGMENTS

This work was supported in part by a grant from the Natural Sciences and Engineering Research Council of Canada. Acknowledgment is made to the donors of The Petroleum Research Fund, administered by the ACS, for partial support of this research and to the European Science Foundation through the SIMU program. We would like to thank Nancy Makri for a critical reading of the manuscript and for producing and supplying the numerical results on the spin-boson model. We would also like to thank Steve Nielsen for discussions and help in the course of this work. The visiting program of the Commissione Calcolo of INFM is acknowledged for supporting an extended visit of R.K. to Rome.

[1] M. F. Herman, Annu. Rev. Phys. Chem. **45**, 83 (1994).

[2] J. C. Tully, in *Modern Methods for Multidimensional Dynamics Computations in Chemistry*, edited by D. L. Thompson (World Scientific, New York, 1998), p. 34.

[3] I. V. Aleksandrov, Z. Naturforsch. A **36a**, 902 (1981).

[4] W. Boucher and J. Traschen, Phys. Rev. D **37**, 3522 (1988).

[5] W. Y. Zhang and R. Balescu, J. Plasma Phys. **40**, 199 (1988); R. Balescu and W. Y. Zhang, *ibid.* **40**, 215 (1988).

[6] O. V. Prezhdo and V. V. Kisil, Phys. Rev. A **56**, 162 (1997).

[7] C. C. Martens and J.-Y. Fang, J. Chem. Phys. **106**, 4918 (1996); A. Donoso and C. C. Martens, J. Phys. Chem. **102**, 4291 (1998).

[8] C. Schütte, preprint SC 99-10 (Konrad-Zuse-Zentrum, 1999).

[9] R. Kapral and G. Ciccotti, J. Chem. Phys. **110**, 8919 (1999).

[10] S. Nielsen, R. Kapral, and G. Ciccotti, J. Chem. Phys. **112**, 6543 (2000); J. Stat. Phys. **101**, 225 (2000).

[11] C. Wan and J. Schofield, J. Chem. Phys. **113**, 7047 (2000).

[12] M. Santer, U. Manthe, and G. Stock, J. Chem. Phys. **114**, 2001 (2001).

[13] A. J. Leggett, S. Chakravarty, A. T. Dorsey, M. P. A. Fisher, A. Garg, and M. Zwerger, Rev. Mod. Phys. **59**, 1 (1987).

[14] U. Weiss, *Quantum Dissipative Systems* (World Scientific, Singapore, 1999).

[15] E. B. Davis, *Quantum Theory of Open Systems* (Academic, London, 1976).

[16] T. Dittrich, P. Hänggi, G.-L. Ingold, B. Kramer, G. Schön, and W. Zwerger, *Quantum Transport and Dissipation* (Wiley, New York, 1998).

[17] J. C. Tully, J. Chem. Phys. **93**, 1061 (1990); Int. J. Quantum Chem. **25**, 299 (1991); S. Hammes-Schiffer and J. C. Tully, J. Chem. Phys. **101**, 4657 (1994); D. S. Sholl and J. C. Tully, *ibid.* **109**, 7702 (1998).

[18] L. Xiao and D. F. Coker, J. Chem. Phys. **100**, 8646 (1994); H. S. Mei and D. F. Coker, *ibid.* **104**, 4755 (1996).

[19] F. Webster, P. J. Rossky, and P. A. Friesner, Comput. Phys. Commun. **63**, 494 (1991); F. Webster, E. T. Wang, P. J. Rossky, and P. A. Friesner, J. Chem. Phys. **100**, 4835 (1994).

[20] D. E. Makarov and N. Makri, Chem. Phys. Lett. **221**, 482 (1994); N. Makri and D. E. Makarov, J. Chem. Phys. **102**, 4600,4611 (1995); N. Makri, J. Math Phys. **36**, 2430 (1995); E. Sim and N. Makri, Computer Phys. Commun. **99**, 335 (1997); N. Makri, J. Phys. Chem. **102**, 4414 (1998).

[21] N. Makri and K. Thompson, J. Phys. Chem. **291**, 101 (1998); K. Thompson and N. Makri, J. Chem. Phys. **110**, 1343 (1999); N. Makri, J. Phys. Chem. **103**, 2823 (1999).

[22] E. P. Wigner, Phys. Rev. **40**, 749 (1932); K. Imre, E. Özimir, M. Rosenbaum, and P. Z. Zwiefel, J. Math. Phys. **5**, 1097 (1967); M. Hillery, R. F. O'Connell, M. O. Scully, and E. P. Wigner, Phys. Rep. **106**, 121 (1984).

[23] B. Shukman, Comput. Phys. Commun. **78**, 279 (1994); W. H. Press, S. A. Teukolsky, W. T. Vetterling, and B. P. Flannery, *Numerical Recipes in C* (Cambridge University Press, Cambridge, 1993); F. J. Hickernell, H. S. Hong, P. L'Ecuyer, and C. Lemieux, SIAM J. Sci. Comput. (USA) **22**, 1117 (2000).

[24] R. P. Feynman and F. L. Vernon, Jr., Ann. Phys. (N.Y.) **24**, 118 (1963).

[25] S. Nielsen, R. Kapral, and G. Ciccotti, J. Chem. Phys. **115**, 5805 (2001).